World Academy of Science, Engineering and Technology
International Journal of Energy and Power Engineering
Vol:13, No:6, 2019

Numerical Study of the Influence of the Primary Stream Pressure on the Performance of the Ejector Refrigeration System Based on Heat Exchanger Modeling

Elhameh Narimani, Mikhail Sorin, Philippe Micheau, Hakim Nesreddine

***Abstract*—**Numerical models of the heat exchangers in ejector refrigeration system (ERS) were developed and validated with the experimental data. The models were based on the switched heat exchangers model using the moving boundary method, which were capable of estimating the zones' lengths, the outlet temperatures of both sides and the heat loads at various experimental points. The developed models were utilized to investigate the influence of the primary flow pressure on the performance of an R245fa ERS based on its coefficient of performance (COP) and exergy efficiency. It was illustrated numerically and proved experimentally that increasing the primary flow pressure slightly reduces the COP while the exergy efficiency goes through a maximum before decreasing.

***Keywords*—**Coefficient of performance, ejector refrigeration system, exergy efficiency, heat exchangers modeling, moving boundary method.

I. Introduction

THE ejector refrigeration cycles are recently used in many engineering applications due to their advantages compared with conventional refrigeration systems: the structural simplicity, low capital cost, the ability to use the inexpensive and free low-grade heat resources like waste heat from various industries and solar energy, to name a few. However, the main drawback of the ejector-based refrigeration cycle is related to its low performance. As a result, it is required to improve the performance of such systems.

Considerable efforts have been made in the literature to investigate the various refrigeration systems numerically and experimentally. It was suggested by several experimental and theoretical studies that performance of the ERS are strongly dependent on the operating conditions of the ejector, evaporator, generator and condenser in the cycle. The most recent findings can be found in the studies conducted by Aphornratana et al. [1], Huang et al. [2] Eames et al. [3], Thongtip and Aphornratana [4], Chen et al. [5].

E. Narimani is studying at Mechanical Engineering Faculty of Université de Sherbrooke, 2500 Boulevard de l'Université, Immeuble K1, Sherbrooke, QC, Canada, J1K 2R1 (phone: +18199191537; e-mail: Elhameh.narimani@Usherbrooke.ca).

M. V. Sorin and P. Micheau are full professors with the Mechanical Engineering Faculty of Université de Sherbrooke, 2500 Boulevard de l'Université, Immeuble K1, Sherbrooke, QC, Canada, J1K 2R1 (e-mail: Mikhail.sorin@Usherbrooke.ca, philippe.micheau@usherbrooke.ca).

H. Nesreddine is with Hydro-Québec, 600 Rue de la Montagne, Shawinigan, QC G9N 7N5, Canada (e-mail: nesreddine.hakim@ireq.ca).

Heat exchangers are considered as crucial components in the ERS modeling. Heat exchangers modeling approaches can be mainly categorized into three groups: 1) single node model or lumped parameter model [6], 2) multi-node model or distributed parameter model [7], and 3) zone model or moving boundary model [8]-[11]. The moving boundary model is widely used to model heat exchangers in transient and steady state conditions due to its high accuracy and low computation time. This model splits a heat exchanger into several regions (based on the number of phases) or Control Volumes (CVs) in which the lumped thermodynamic properties are averaged. The limits of the regions may move between CVs. In spite of the high accuracy of the finite volume or finite difference models, the lumped parameter or moving-boundary method is much faster which is depicted by Grald and MacArthur [12]. The moving-boundary method is considered as an appropriate approach to model the heat exchangers for control purposes. Although the tremendous work performed in this area, some improvements are still required in the moving boundary method. For instance, the significant number of available models assumes the fixed number of zones or the fixed lengths for the zones.

In this work, the numerical investigation of the three heat exchangers used in an ERS was conducted. To develop the steady-state models of the heat exchangers, the ε-NTU model in combination with the moving boundary method was applied. A simple method was presented to evaluate the length of the different zones in the heat exchangers and the simulation results showed a good agreement with experimental data. The developed models could predict the thermal loads and outlet temperatures of the both sides with the errors up to 8.55 % and 6.46 %, respectively.

II. Modeling

The ejector refrigeration cycle includes six components: the generator, condenser, evaporator, ejector, electronic expansion valve and pump. Fig. 1 shows the schematic view of a typical ejector refrigeration system. The value of all the model parameters applied in this study are obtained by employing an R245fa ejector driven refrigeration plant located at LTE center of Hydro-Quebec. EES software was applied to solve the developed equations.

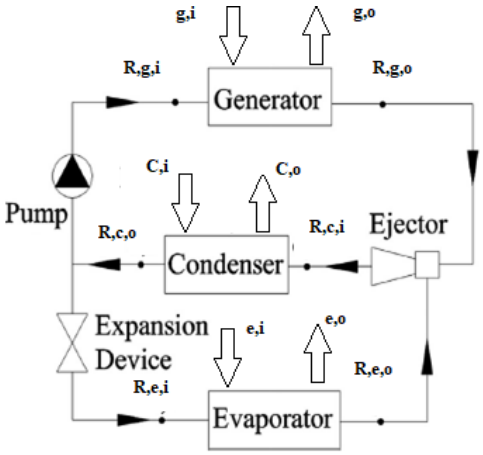

Fig. 1 Schematic representation of an ejector refrigeration circle

The zone model or moving boundary model [8], [9] is widely used to model the heat exchangers in transient and steady state conditions. In the present study, the moving boundary model is applied to model the heat exchangers. The values of the thermal loads in the evaporating, preheating, condensing and desuperheating regions of the generator, evaporator and condenser can be evaluated using the heat exchangers' pressure and inlet temperatures of the both sides and compared with their equivalent values calculated by $\varepsilon - NTU$ method. The equations applied to model the heat exchangers are listed in Appendix.

The relation introduced by Gnielinski [13]-[15] was used to evaluate the convective heat transfer coefficients in single-phase regions. The heat transfer coefficients of the evaporation zones (in the generator and evaporator) are calculated using the correlation introduced by Yan and Lin [10]. Furthermore, the heat transfer coefficient of the condensation zone of the condenser is estimated by Yan et al. correlation [10]. Figs. 2-4 depict the heat transfer diagram along the heat exchangers.

It was assumed that the heat transfer areas in the three heat exchangers are divided into three zones in the generator and the condenser while the evaporator is represented by two zones. The heat transfer area of each region is a portion of the total heat transfer area of the corresponding heat exchanger defined by dimensionless length factors. For instance, length factors of the preheating (η_{ph}) and evaporating (η_{ev}) zones are calculated in the iterative solutions based on which the heat transfer rates in the preheating and evaporation zones are evaluated using (5) and (6). The h_{fg} represents the vaporization enthalpy of the refrigerant at the generator pressure Pg. In each iteration, the evaluated values of $\dot{Q}_{ev}$and $\dot{Q}_{ph}$ are compared to their real values calculated by (5) and (6) and the estimated values of η_{ph} and η_{ev} are renewed until convergence is reached. The same method is used for the condenser and evaporator. All the used equations are listed in Table I.

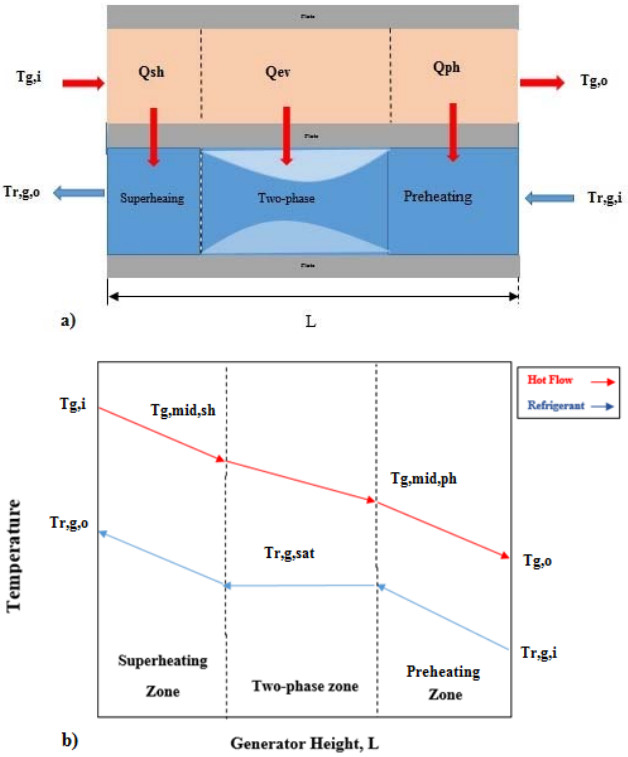

Fig. 2 (a) Heat transfer along the three zones of the generator (b) thermal plan of both sides

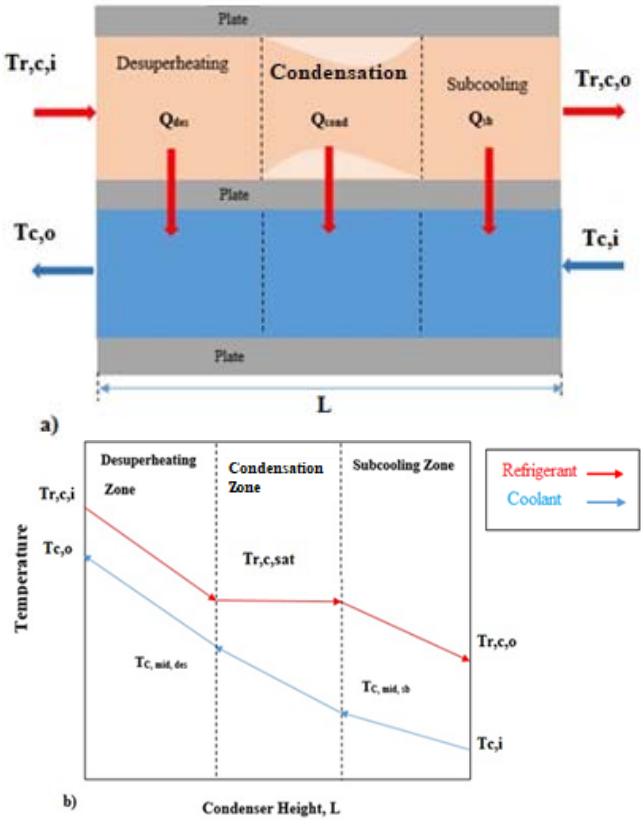

Fig. 3 (a) Heat transfer diagram along the three zones of condenser (b) thermal plan of both sides

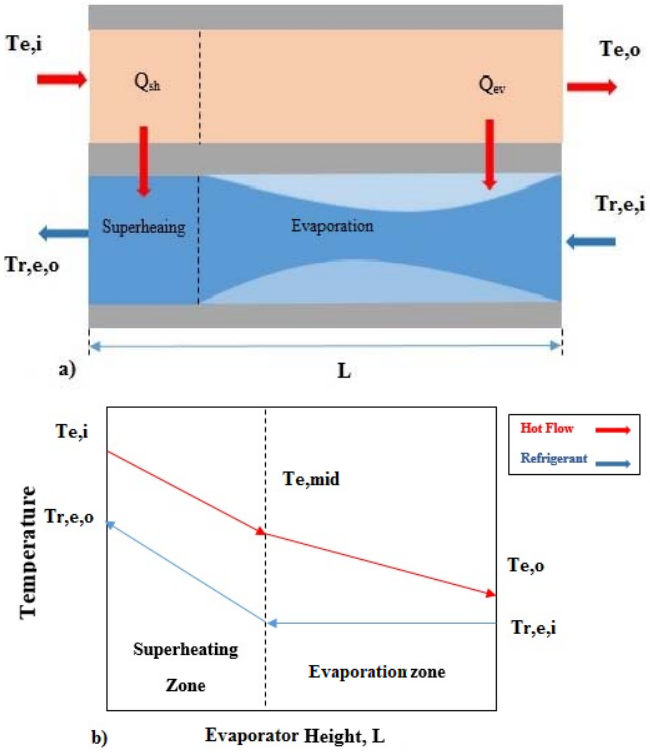

Fig. 4 (a) Heat transfer diagram along the evaporator's two zones (b) thermal plan of both sides

III. Results and Discussion

In order to validate the model, experimental data obtained by Hamzaoui et al. [16] were used. The primary flow pressure is chosen as a disturbance to validate the developed models. The interval of variation ranges from 484 kPa to 538 kPa.

TABLE I
GOVERNING EQUATIONS IN THE HEAT EXCHANGERS

Generator	Equations	No.
	$U = \frac{1}{\frac{1}{h_{r,g}} + \frac{1}{h_g}}$	(1)
Superheating Zone	$\dot{C}_{r,g,sh} = (\dot{m}C_P)_{r,g,sh}$ $\dot{C}_{g,sh} = (\dot{m}C_P)_{g,sh}$ $\dot{C}_{Min,sh} = \text{minimum}(\dot{C}_{r,g,sh}, \dot{C}_{g,sh})$ $\dot{C}_{Max,sh} = \text{maximum}(\dot{C}_{r,g,sh}, \dot{C}_{g,sh})$ $C_{sh} = \frac{\dot{C}_{Min,sh}}{\dot{C}_{Max,sh}}$ $A_{sh} = A\eta_{sh}$ $UA_{sh} = U_{sh}A_{sh}$ $NTU_{sh} = UA_{sh}/\dot{C}_{Min,sh}$ $\dot{Q}_{sh} = \varepsilon_{sh}\dot{C}_{Min,sh}(T_{g,in} - T_{r,g,sat})$ $T_{g,mid,sh} = T_{g,in} - \frac{\dot{Q}_{sh}}{\dot{C}_{g,sh}}$ $T_{r,g,out} = \dot{Q}_{sh}/\dot{C}_{r,g,sh} + T_{r,g,sat}$	(2)
Evaporation Zone	$\dot{C}_{r,g,ev} = (\dot{m}C_P)_{r,g,ev}$ $\dot{C}_{g,ev} = (\dot{m}C_P)_{g,ev}$ $C_{ev} = \{\text{phase change}\} = 0$ $A_{ev} = A\eta_{ev}$ $UA_{ev} = U_{ev}A_{ev}$ $NTU_{ev} = \frac{UA_{ev}}{\dot{C}_{g,ev}}$ $\dot{Q}_{ev} = \varepsilon_{ev}\dot{C}_{g,ev}(T_{g,mid,sh} - T_{r,g,sat})$ $T_{g,mid,ph} = T_{g,mid,sh} - \frac{\dot{Q}_{ev}}{\dot{C}_{g,ev}}$	(3)
Preheating zone	$\dot{C}_{r,g,ph} = (\dot{m}C_P)_{r,g,ph}$ $\dot{C}_{g,ph} = (\dot{m}C_P)_{g,ph}$ $\dot{C}_{Min,ph} = \text{minimum}(\dot{C}_{r,g,ph}, \dot{C}_{g,ph})$ $\dot{C}_{Max,ph} = \text{maximum}(\dot{C}_{r,g,ph}, \dot{C}_{g,ph})$ $C_{ph} = \frac{\dot{C}_{Min,ph}}{\dot{C}_{Max,ph}}$ $A_{ph} = A\eta_{ph}$ $UA_{ph} = U_{ph}A_{ph}$ $NTU_{ph} = \frac{UA_{ph}}{\dot{C}_{Min,ph}}$ $\dot{Q}_{ph} = \varepsilon_{ph}\dot{C}_{Min,ph}(T_{g,mid,ph} - T_{r,g,i})$ $T_{g,o} = T_{g,mid,ph} - \dot{Q}_{ph}/\dot{C}_{g,ph}$	(4)
	$\dot{Q}_{ph,c} = (\dot{m}C_P)_{r,g,ph}(T_{r,g,sat} - T_{r,g,i})$	(5)
	$\dot{Q}_{total} = \dot{Q}_{ph} + \dot{Q}_{ev} + \dot{Q}_{sh}$	(6)
Condenser	**Equations**	**No.**
Subcooling Zone	$\dot{C}_{r,c,sb} = (\dot{m}C_P)_{r,c,sb}$ $\dot{C}_{c,sb} = (\dot{m}C_P)_{c,sb}$ $\dot{C}_{Min,sb} = \text{minimum}(\dot{C}_{r,c,sb}, \dot{C}_{c,sb})$ $\dot{C}_{Max,sb} = \text{maximum}(\dot{C}_{r,c,sb}, \dot{C}_{c,sb})$ $C_{sb} = \frac{\dot{C}_{Min,sb}}{\dot{C}_{Max,sb}}$ $A_{sb} = A\eta_{sb}$ $UA_{sb} = U_{sb}A_{sb}$ $NTU_{sb} = \frac{UA_{sb}}{\dot{C}_{Min,sb}}$ $\dot{Q}_{sb} = \varepsilon_{sb}\dot{C}_{Min,sb}(T_{r,c,sat} - T_{c,i})$ $T_{c,mid,sb} = T_{c,i} + \frac{\dot{Q}_{sb}}{\dot{C}_{c,sb}}$ $T_{r,c,o} = T_{r,c,sat} - \frac{\dot{Q}_{sb}}{\dot{C}_{r,c,sb}}$	(7)
Condensation Zone	$\dot{C}_{r,c,cond} = (\dot{m}C_P)_{r,c,cond}$ $\dot{C}_{c,cond} = (\dot{m}C_P)_{c,cond}$ $C_{cond} = \{\text{phase change}\} = 0$ $A_{cond} = A\eta_{cond}$ $UA_{cond} = U_{cond}A_{cond}$ $NTU_{cond} = \frac{UA_{cond}}{\dot{C}_{c,cond}}$ $\dot{Q}_{Cond} = \varepsilon_{cond}\dot{C}_{c,cond}(T_{r,c,sat} - T_{c,mid,sb})$ $T_{c,mid,des} = T_{c,mid,sb} + \frac{\dot{Q}_{Cond}}{\dot{C}_{c,cond}}$	(8)
De-superheating Zone	$\dot{C}_{r,c,des} = (\dot{m}C_P)_{r,c,des}$ $\dot{C}_{c,des} = (\dot{m}C_P)_{c,des}$ $\dot{C}_{Min,des} = \text{minimum}(\dot{C}_{r,c,des}, \dot{C}_{c,des})$ $\dot{C}_{Max,des} = \text{maximum}(\dot{C}_{r,c,des}, \dot{C}_{c,des})$ $C_{des} = \frac{\dot{C}_{Min,des}}{\dot{C}_{Max,des}}$ $A_{des} = A\eta_{des}$ $UA_{des} = U_{des}A_{des}$ $\dot{Q}_{des} = \varepsilon_{des}\dot{C}_{Min,des}(T_{r,c,i} - T_{C,mid.des})$ $T_{c,o} = T_{c,mid.des} + \frac{\dot{Q}_{des}}{\dot{C}_{c,des}}$	(9)
	$\dot{Q}_{des,c} = (\dot{m}C_P)_{r,c,des}(T_{r,c,sat} - T_{r,c,i})$	(10)
	$\dot{Q}_{total} = \dot{Q}_{des} + \dot{Q}_{cond} + \dot{Q}_{sb}$	(11)
Evaporator	**Equations**	**No.**
Superheating Zone	$\dot{C}_{r,e,sh} = (\dot{m}C_P)_{r,e,sh}$ $\dot{C}_{e,sh} = (\dot{m}C_P)_{e,sh}$ $\dot{C}_{Min,sh} = \text{minimum}(\dot{C}_{r,e,sh}, \dot{C}_{e,sh})$ $\dot{C}_{Max,sh} = \text{maximum}(\dot{C}_{r,e,sh}, \dot{C}_{e,sh})$ $C_{sh} = \frac{\dot{C}_{Min,sh}}{\dot{C}_{Max,sh}}$ $A_{sh} = A\eta_{sh}$ $UA_{sh} = U_{sh}A_{sh}$ $NTU_{sh} = \frac{UA_{sh}}{\dot{C}_{Min,sh}}$	(12)

	$\dot{Q}_{sh} = \varepsilon_{sh}\dot{C}_{Min,sh}(T_{e,i} - T_{r,e,sat})$ $T_{e,mid} = T_{e,i} - \dot{Q}_{sh}/\dot{C}_{Min,sh}$ $T_{r,e,o} = \dot{Q}_{sh}/\dot{C}_{r,e,sh} + T_{r,g,sat}$	
Evaporation Zone	$\dot{C}_{r,e,ev} = (\dot{m}C_P)_{r,e,ev}$ $\dot{C}_{e,ev} = (\dot{m}C_P)_{e,ev}$ $C_{ev} = \{\text{phase change}\} = 0$ $A_{ev} = A\eta_{ev}$ $UA_{ev} = U_{ev}A_{ev}$ $NTU_{ev} = \frac{UA_{ev}}{\dot{C}_{e,ev}}$ $\dot{Q}_{ev} = \varepsilon_{ev}\dot{C}_{e,ev}(T_{e,mid} - T_{r,e,sat})$ $T_{e,o} = T_{e,mid} - \frac{\dot{Q}_{ev}}{\dot{C}_{e,ev}}$	(13)
	$\dot{Q}_{total} = \dot{Q}_{ev} + \dot{Q}_{sh}$	(14)

A. Effect of the Primary Flow Pressure on Heat Transfer

Fig. 5 shows the comparison between numerical and experimental ERS performance based on COP, which is defined as:

$$COP = \frac{\dot{Q}_e}{\dot{Q}_g} \tag{17}$$

It is observed that generally the COP decreases with an increase in the primary flow pressure. This is because the cooling load in the evaporator is kept constant while the thermal input at the generator increases with a rise in the primary flow pressure as presented in Fig. 6.

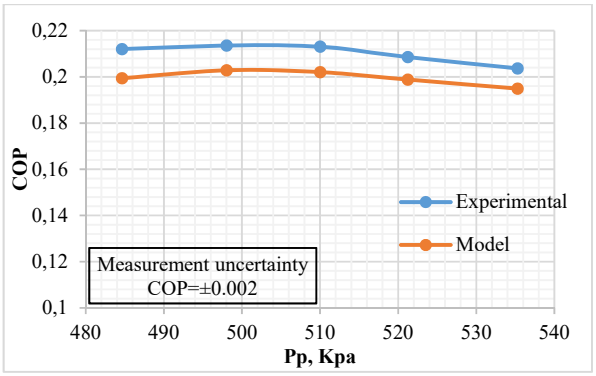

Fig. 5 Variation of the COP the primary flow pressure

Fig. 7 shows the influences of the primary flow rate on the predicted thermal conductance UA of the evaporator and generator. It can be seen that the UA increases linearly as a function of the primary flow pressure. However, in the evaporator, there is an optimum primary flow pressure where the minimum UA can be obtained. It can be explained by the fact that the primary mass flow rate in the generator and the heat transfer rate both increase while the temperature difference between two sides decreases with rising the primary flow pressure and consequently, UA increases sharply. On the other hand, in evaporator, the mass flow rate of the secondary stream are kept constant and the UA is strongly dependent on the logarithmic temperature difference (ΔT_{lmtd}) between the two sides and the thermal load, which rises to a maximum point then decreases with augmenting the primary flow rate (Fig. 8).

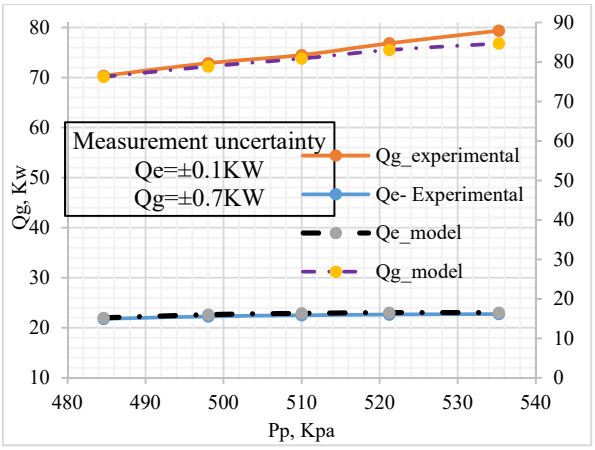

Fig. 6 Variations of $\dot{Q}_e, \dot{Q}_g$ with the primary flow pressure

It is believed that the minimum logarithmic temperature difference in the evaporator is related to the minimum evaporation pressure (secondary pressure) at the same point, which is shown in Fig. 9. The thermal conductance can be crucial from the point of view of the fixed costs and the size of the refrigeration system. The larger the UA, the larger heat exchanger is required.

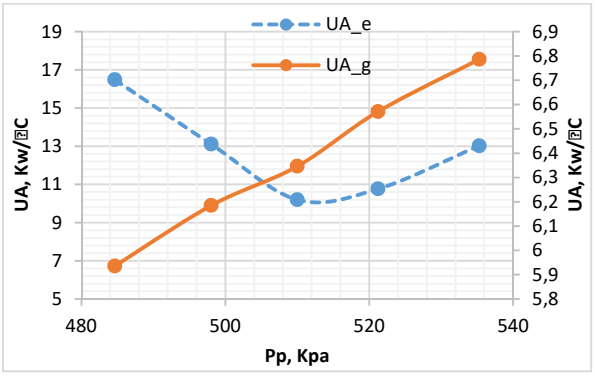

Fig. 7 Variations of UA in the generator and evaporator with the primary flow pressure

B. Effect of the Primary Flow Rate on the Exergy Efficiency (η_{II}) of the ERS

The exergy analysis of the ERS system can be beneficial to evaluate the irreversibility decrease for the cycle. Here, the exergy efficiency is used as another indicator to demonstrate the efficiency of the ERS defined as follows [17]:

$$\eta_{II} = \frac{E_e}{E_g + W_g} \tag{18}$$

where E_e, E_g and W_g are exergy of heat rates in the evaporator and generator and pump work, respectively. The pump work is negligible and is not included in the exergy efficiency calculations. To evaluate the exergy of the heat rate the following equations are used:

$$E_e = \dot{Q}_e \left|1 - \frac{T_r}{T_{sc,e}}\right| \tag{19}$$

$$E_g = \dot{Q}_g \left|1 - \frac{T_r}{T_{sc,g}}\right| \quad (20)$$

$$T_{sc,e} = \frac{T_{e,i}+T_{e,o}}{2} \quad (21)$$

$$T_{sc,g} = \frac{T_{g,i}+T_{g,o}}{2} \quad (22)$$

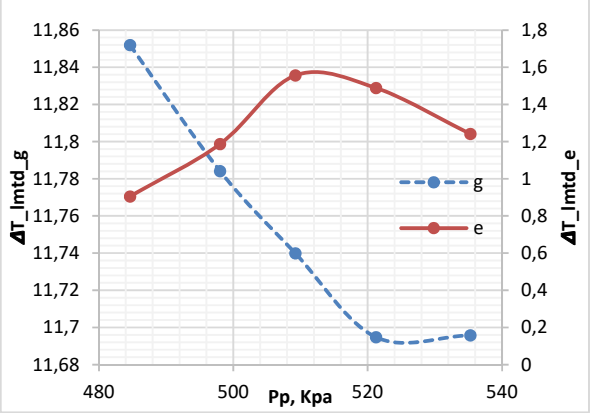

Fig. 8 Variations of ΔT_{lmtd} in the generator and evaporator with the primary flow pressure

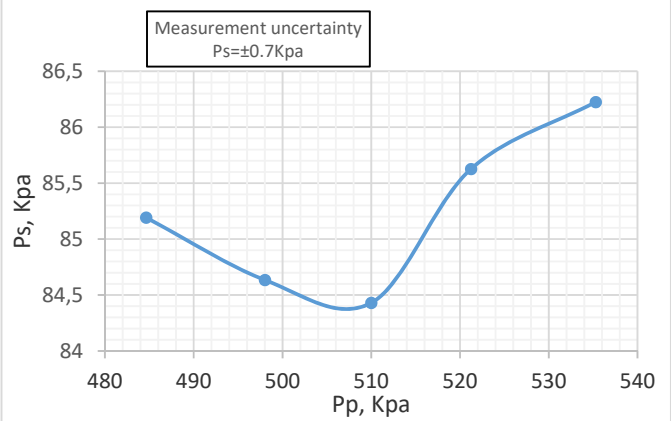

Fig. 9 Variation of the Secondary Stream Pressure (PS) with the primary stream pressure (Pp)

Tr is the surrounding temperature. The second law or exergy efficiency of the cycle is evaluated using the following formula:

$$\eta_{II} = \frac{\dot{Q}_e\left|1-\frac{T_r}{T_{sc,e}}\right|}{\dot{Q}_g\left|1-\frac{T_r}{T_{sc,g}}\right|} = COP\frac{\left|1-\frac{T_r}{T_{sc,e}}\right|}{\left|1-\frac{T_r}{T_{sc,g}}\right|} \quad (23)$$

Fig. 10 depicts the influence of the increase of the primary flow pressure on the exergy efficiency. With the rise in the primary pressure the exergy efficiency increases initially to a maximum and then decreases. The reason can be explained based on the variation of COP with the primary flow pressure and the second factor of the Eq. (23). The COP decreases with augmenting the primary flow pressure, however, the second term of the Eq. (23) first increases slightly and then decreases with rising the primary pressure.

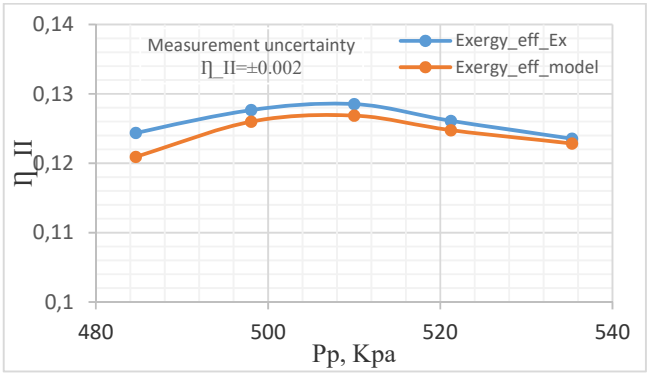

Fig. 10 Effect of the primary flow pressure on the exergy efficiency

IV. Conclusion

In the present study, the steady state models of the heat exchangers in an ERS using R245fa refrigerant were developed with EES software. The Moving Boundary method was utilized to study the heat exchangers by calculating the thermal loads, the outlet temperatures of both sides and length factors of various zones at different operation conditions. The proposed model was validated with experimental data, which showed a good agreement. The developed model was used to predict the impact of the primary flow pressure on the COP and η_{II} and it was revealed that increasing the primary flow pressure results in COP drop while η_{II} rises to a maximum point before decreasing.

Appendix

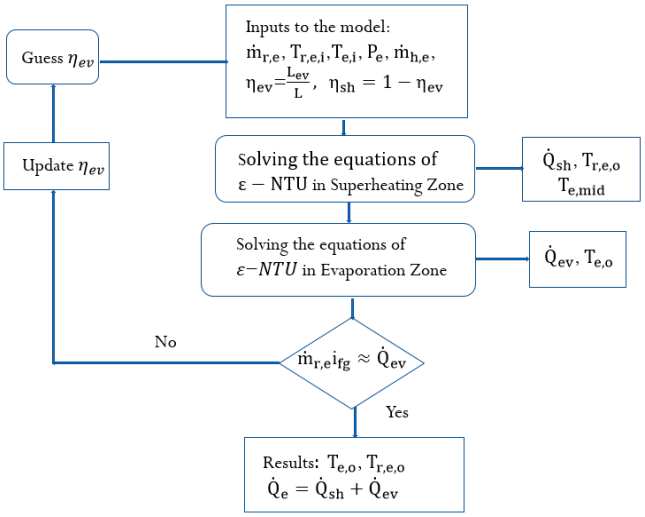

Fig. 11 Solution algorithm flow chart for the evaporator model

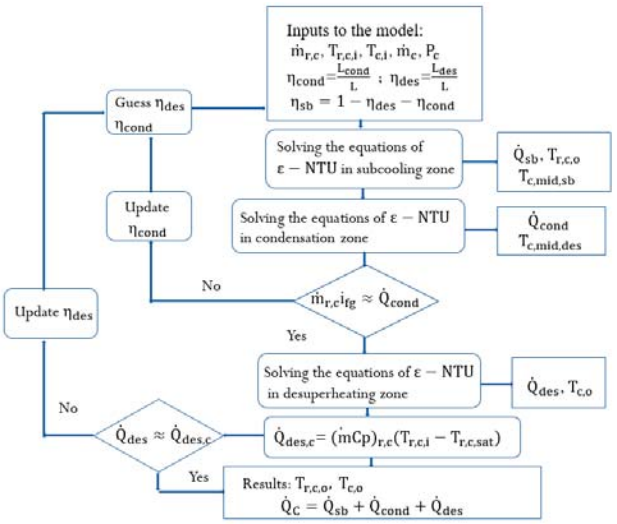

Fig. 12 Solution algorithm flow chart for the condenser model

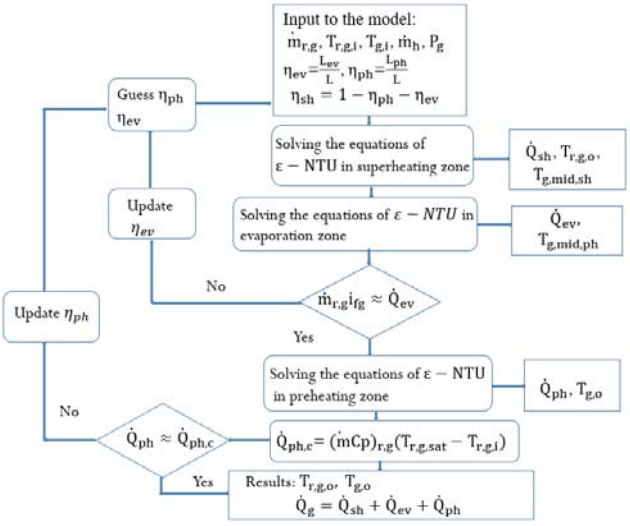

Fig. 13 Solution algorithm flow chart for the generator model

ACKNOWLEDGMENT

This project is a part of the Collaborative Research and Development (CRD) Grants Program at 'Université de Sherbrooke'. The authors acknowledge the support of the Natural Sciences and Engineering Research Council of Canada, Hydro-Québec, Rio Tinto, Alcan and Canmet ENERGY Research Center of Natural Resources Canada

NOMENCLATURE

Symbol	Definition
P	Pressure, Kpa
h	Enthalpy, kj/kg
$\dot{m}$	Mass flow rate, kg/s
A	Surface area, m2
T	Temperature, °C
$\dot{Q}$	Heat load, KW/s
C	Capacity ratio
$\dot{C}$	Capacitance rate, Kj/s.°C
C_p	Specific heat, Kj/kg.°C
ε	effectiveness factor
COP	coefficient of performance
U	overall heat transfer coefficient, kw/m^2. °C
i_{fg}	latent heat of vaporization (condensation) at the heat exchanger pressure, Kj/Kg

Greek characters

ρ	Density, kg/m^3
η_{II}	Second-law efficiency
η_{sh}	Length factor for superheating area
η_{ev}	Length factor for evaporation area
η_{ph}	Length factor for preheating area
η_{des}	Length factor for desuperheating area
η_{cond}	Length factor for condensation area
η_{sb}	Length factor for subcooling area

REFERENCES

[1] Aphornratana S, Chungpaibulpatana S, Srikhirin P. Experimental investigation of an ejector refrigerator: Effect of mixing chamber geometry on system performance. Int J Energy Res 2001; 25:397–411. doi:10.1002/er.689.
[2] Huang BJ, Jiang CB, Hu FL. Ejector Performance Characteristics and Design Analysis of Jet Refrigeration System. J Eng Gas Turbines Power 1985; 107:792. doi:10.1115/1.3239802.
[3] I. W. Eames, S. Aphornratana, H. Haider. A theoretical and experimental study of a small scale steam jet refrigerator. Int J Refrig 1995; 18:378–86. doi:10.1016/0140-7007(95)98160-M.
[4] Thongtip T, Aphornratana S. An experimental analysis of the impact of primary nozzle geometries on the ejector performance used in R141b ejector refrigerator. Appl Therm Eng 2017; 110:89–101. doi:10.1016/j.applthermaleng.2016.08.100.
[5] Chen W, Shi C, Zhang S, Chen H, Chong D, Yan J. Theoretical analysis of ejector refrigeration system performance under overall modes. Appl Energy 2015:1–11. doi:10.1016/j.apenergy.2016.01.103.
[6] Kays WM, London AL. Compact Heat Exchangers. 3rd ed. 1997.
[7] Liu J, Wei W, Ding G, Zhang C, Fukaya M, Wang K, et al. A general steady state mathematical model for fin-and-tube heat exchanger based on graph theory. Int J Refrig 2004; 27:965–73. doi:10.1016/j.ijrefrig.2004.06.008.
[8] Costa MLM, Parise JAR. A Three-Zone Simulation Model for Air-Cooled Condensers 1993; 13:97–113.
[9] Ge YT, Cropper R. Performance evaluations of air-cooled condensers using pure and mixture refrigerants by four-section lumped modelling methods. Appl Therm Eng 2005; 25:1549–64. doi:10.1016/j.applthermaleng.2004.10.001.
[10] Ding G liang. Recent developments in simulation techniques for vapour-compression refrigeration systems. Int J Refrig 2007; 30:1119–33. doi:10.1016/j.ijrefrig.2007.02.001.
[11] Bejarano G, Alfaya JA, Ortega MG, Vargas M. On the difficulty of globally optimally controlling refrigeration systems. Appl Therm Eng 2017; 111:1143–57. doi:10.1016/j.applthermaleng.2016.10.007.
[12] Grald EW, MacArthur JW. A moving-boundary formulation for modeling time-dependent two-phase flows. Int J Heat Fluid Flow 1992; 13:266–72.
[13] Seyfettin Yildiz. Design and Simulation of a Vapor Compression Refrigeration Cycle for a Micro Refrigerator. Middle East Technical University, 2010.
[14] Admiraal DM, Bullard CW. Heat Transfer in Refrigerator Condensers and Evaporators. vol. 61801. Illinois, Urbana: 1993.
[15] Gullapalli VS. Estimation of Thermal and Hydraulic Characteristics of Compact Brazed Plate Heat Exchangers. Lund University, 2013.
[16] Hamzaoui M, Nesreddine H, Aidoun Z, Balistrou M. Experimental study of a low grade heat driven ejector cooling system using the working fluid R245fa. Int J Refrig 2018; 86:388–400. doi:10.1016/j.ijrefrig.2017.11.018.
[17] Eldakamawy MH, Sorin M V, Brouillette M. Energy and exergy investigation of ejector refrigeration systems using retrograde refrigerants. Int J Refrig 2017; 78:176–92. doi:10.1016/j.ijrefrig.2017.02.031.